JGR Atmospheres

RESEARCH ARTICLE
10.1029/2022JD036567

Special Section:
Atmospheric PM2.5 in China: physics, chemistry, measurements, and modeling

Long-Term Evolution of Particulate Nitrate Pollution in North China: Isotopic Evidence From 10 Offshore Cruises in the Bohai Sea From 2014 to 2019

Zheng Zong[1,2,3], Chongguo Tian[1,3], Zeyu Sun[1,3], Yang Tan[1,3], Yajun Shi[1,3], Xiaohuan Liu[4], Jun Li[5], Yunting Fang[6], Yingjun Chen[7], Yuhao Ma[8], Huiwang Gao[4], Gan Zhang[5], and Tao Wang[2]

[1]CAS Key Laboratory of Coastal Environmental Processes and Ecological Remediation, Shandong Key Laboratory of Coastal Environmental Processes, Yantai Institute of Coastal Zone Research (YIC), Chinese Academy of Sciences (CAS), YICCAS, Yantai, China, [2]Department of Civil and Environmental Engineering, Hong Kong Polytechnic University, Hong Kong, China, [3]Center for Ocean Mega-Science, Chinese Academy of Sciences, Beijing, China, [4]Key Laboratory of Marine Environment and Ecology, Ministry of Education, Ocean University of China, Qingdao, China, [5]State Key Laboratory of Organic Geochemistry and Guangdong Key Laboratory of Environmental Protection and Resources Utilization, Guangzhou Institute of Geochemistry, Chinese Academy of Sciences, Guangzhou, China, [6]CAS Key Laboratory of Forest Ecology and Management, Institute of Applied Ecology, Chinese Academy of Sciences, Shenyang, China, [7]Shanghai Key Laboratory of Atmospheric Particle Pollution and Prevention (LAP3), Department of Environmental Science and Engineering, Fudan University, Shanghai, China, [8]Shenzhen Engn Lab Microalgal Bioenergy, Harbin Institute of Technology Harbin Inst Technol Shenzhen, Shenzhen, China

Key Points:

- Although the concentration of particulate has decreased in North China, the proportion of nitrate has increased significantly
- The increase of atmospheric oxidation promotes the formation of nitrate, greatly offsetting China's efforts to reduce nitrogen oxides emission
- The contribution of coal combustion to the nitrate has dropped, but that of microbial processes has risen the most

Supporting Information:

Supporting Information may be found in the online version of this article.

Correspondence to:

C. Tian,
cgtian@yic.ac.cn

Citation:

Zong, Z., Tian, C., Sun, Z., Tan, Y., Shi, Y., Liu, X., et al. (2022). Long-term evolution of particulate nitrate pollution in North China: Isotopic evidence from 10 offshore cruises in the Bohai Sea from 2014 to 2019. *Journal of Geophysical Research: Atmospheres*, *127*, e2022JD036567. https://doi.org/10.1029/2022JD036567

Received 27 JAN 2022
Accepted 23 MAY 2022

Abstract Atmospheric nitrate (NO_3^-) pollution has become an obstacle to efforts to further reduce fine particulate ($PM_{2.5}$) concentration in North China. However, there have been limited long-term measurements of NO_3^- and isotopic knowledge ($\delta^{15}N$, $\delta^{18}O$) on the driving factors during NO_3^- changes. Here, we report observations of 10 voyages from 2014 to 2019 conducted in the Bohai Sea, a typical background area in North China. The results show that the average proportion of NO_3^- in $PM_{2.5}$ increased from 0.08 to 0.16 over the study period. The $\delta^{15}N$–NO_3^- ranged from −4.1‰ to +20.5‰, with a significant annual decline ($p < 0.01$), especially in winter. The average $\delta^{18}O$–NO_3^- was +72.6 ± 13.5‰, and a Monte Carlo calculation revealed that the contribution of the •OH pathway in the NO_3^- formation declined by 27.4% in winter, implying an increase in O_3 pollution. Coal combustion remained the most important contributor to NO_3^- (46.6 ± 15.9%), but its contribution showed a significant downward trend ($p < 0.01$), consistent with the control of disperse coal use in North China. Enhancement of atmospheric oxidation and the unexpected large increase in contribution of microbial processes were found to be the main causes of the increasingly serious NO_3^- pollution in North China. In addition, a spike in the contribution of coal combustion in 2018 indicates that the coal-control policy needs to be reinforced.

Plain Language Summary In North China where winter haze events still occur frequently, nitrate (NO_3^-) has replaced sulfate (SO_4^{2-}) as the most important component in particulate pollution. Therefore, it is very important to explore the sources and formation mechanisms of NO_3^- and to evaluate their changes in recent years. In this study, multi-year offshore observations were conducted in the Bohai Sea that is surrounded by densely populated, industrialized, and agriculture-intensive land areas of North China. The sources and formation of NO_3^- were apportioned based on the isotope technique ($\delta^{15}N$ and $\delta^{18}O$) and Bayesian model. We find that the atmospheric NO_3^- pollution was becoming serious, despite the decrease in fine particulate concentration. Coal combustion was the most important contributor of NO_3^-, however, it has showed a significant downward trend ($p < 0.01$). The increase of atmospheric oxidation was the primary reason for the increasingly serious NO_3^- pollution, which offsets the efforts of reducing nitrogen oxides (NO_x) emissions. In addition, the unexpected large increase in contribution of microbial processes could be another important factor. This study highlights the importance to consider the increases in atmospheric oxidation and microbial NO_x emission in formulating effective strategies to mitigate the serious NO_3^- pollution in North China.

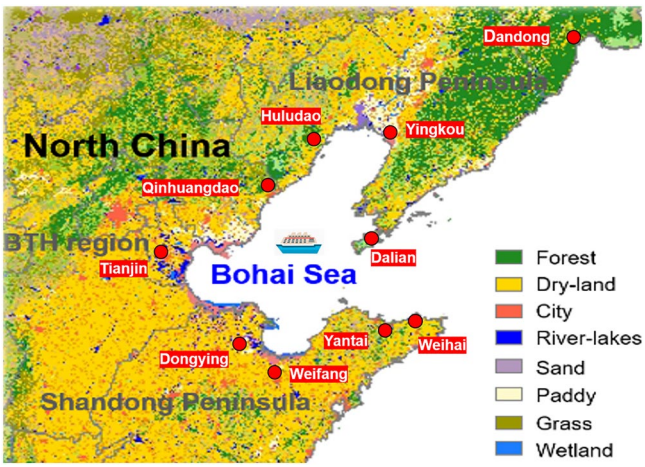

Figure 1. The geographical locations of the Bohai Sea and 10 representative cities selected to assess the average atmospheric NO_2 and O_3 concentrations during the sampling period.

1. Introduction

With the implementation of strict air-pollution control policies in North China, the concentration of atmospheric fine particulate matter ($PM_{2.5}$) has declined in recent years (Zhang & Geng, 2019). However, few studies on multiple-year observation data have shown that the composition of $PM_{2.5}$ in Beijing and the several other cities in the North China Plain has undergone significant changes; the nitrate (NO_3^-) concentration and its proportion in $PM_{2.5}$ have increased despite reductions of nitrogen oxides (NO_x) emissions (Fan et al., 2020; Fu et al., 2020; Li, Gao, et al., 2021; Li, Ma, et al., 2021; Li, Wu, et al., 2021). In fact, NO_3^- has replaced sulfate (SO_4^{2-}) as the most important component in particulate pollution in North China (Fu et al., 2020; Luo et al., 2019, 2021; Song et al., 2019). Therefore, the NO_3^- has become a major obstacle to further reducing $PM_{2.5}$ concentration in North China.

Atmospheric NO_3^- is mainly produced from the secondary conversion of NO_x, and is then removed from the atmosphere by deposition processes (Hastings et al., 2003; Li, Gao, et al., 2021; Li, Ma, et al., 2021; Li, Wu, et al., 2021; Zhao et al., 2015). Thus, the NO_3^- concentration is closely related to the NO_x emission intensity, NO_3^- formation mechanisms, and NO_3^- deposition. As reported, NO_x emissions from anthropogenic sources have decreased since 2011 (Liu et al., 2017). Regarding the NO_3^- formation mechanisms, Fu et al. (2020) suggests that the increasing oxidants (i.e., O_3 and •OH) was the main reason for the increasing level of winter NO_3^- in the North China Plain based on Community Multiscale Air Quality (CMAQ) model. The ammonia-rich environment in North China could promote the conversion of nitric acid to NO_3^- (Gu et al., 2022; Peng at al., 2021; Xu et al., 2019). In addition, another study using the GEOS-Chem atmospheric chemistry model has suggested that the high and increasing NO_3^- concentration in the North China Plain can be attributed to the weakening of deposition processes (Zhai et al., 2021). However, there have been few reports of long-term and regional measurements of NO_3^- in North China, especially the investigations of the sources and formation of NO_3^- based on the isotopic observation data. This greatly limits our understanding of the evolution of NO_3^- in North China.

The Bohai Sea is adjacent to the Beijing-Tianjin-Hebei region, Shandong Peninsula, and Liaodong Peninsula (Figure 1), all of which are land areas with intense human activities (Zhang, Guan, et al., 2020). Influenced by the Asian monsoon, the Bohai Sea is a receiver of the mixed pollution from these areas (Zong et al., 2018). Furthermore, there is no obvious source of anthropogenic emissions of its own, except emissions from ships; the Bohai Sea can be considered a typical background area in North China. For example, a previous study suggests that ship emissions contributed less than 3% to the total $PM_{2.5}$ in the Bohai Sea (Zhang et al., 2014).

In the present study, the Bohai Sea was selected as the study region to explore the evolutionary characteristics of NO_3^- in North China. Specifically, multi-year offshore observations were conducted in this region, and the sources and formation of NO_3^- were apportioned based on the stable isotope analysis ($\delta^{15}N$ and $\delta^{18}O$; Text S1; Table S1 in Supporting Information S1). In addition, Bayesian model was adopted to further achieve the quantitative apportionment. The main goals of this research were to (a) document the changes of NO_3^- in $PM_{2.5}$ from 2014 to 2019; (b) understand the sources and formation of NO_3^- based on $\delta^{15}N$–$NO_3^-$and $\delta^{18}O$–NO_3^-; (c) quantify the annual variation of sources and formation of NO_3^-; (d) identify the driving factors of the aggravation of NO_3^- pollution in North China.

2. Materials and Methods

2.1. Sampling Campaign and Data Collection

The observations were made during 10 cruises in the Bohai Sea from 2014 to 2019 (Figure S1; Table S2 in Supporting Information S1), with the aim of exploring the regional evolution of NO_3^- in North China. The observations were mainly concentrated in the summer (average temperature: 23.5 ± 1.8°C) and winter (3.8 ± 3.5°C), which are the seasons in which the characteristics of air pollution are typically studied. (Yang et al., 2021). A high-volume sampler (Tisch Environmental, Cleves, OH, USA) was operated at 1.13 m^3 min^{-1} to collect $PM_{2.5}$

samples on quartz fiber filters (QM-A; Whatman, Maidstone, UK; preheated for 5 hr at 450°C). The sampler with temperature sensor was installed on the top tower of the ship, and a total of 98 $PM_{2.5}$ samples and 12 blank samples were collected only when cruising against the wind to avoid contamination from the vessel's own emissions (Luo et al., 2018). After collection, the filters were stored in a freezer at −20°C until analysis. Before and after each sampling, the filter was allowed to equilibrate at 25°C for 24 hr, at a relative humidity of 39%, and was then weighed using an MC5 electronic microbalance (±10 μg; Sartorius, Göttingen, Germany) to determine the $PM_{2.5}$ concentration. Each weighing was repeated at least three times, with the difference being ≤10 μg for the blank filters (12 samples) and ≤20 μg for the sampled filters (98 samples). In addition, this study selected 10 representative cities (Weihai, Yantai, Weifang, Dongying, Tianjin, Qinhuangdao, Huludao, Yingkou, Dalian, Dantong; Figure 1) around the Bohai Sea and counted their NO_2 and O_3 concentrations reported (https://www.aqistudy.cn/historydata/) to represent the average feature of these pollutants in the Bohai Sea during the sampling period.

2.2. Chemistry and Isotope Analysis

One 47-mm diameter punch was removed from the sampled filters and subjected to Milli-Q water extraction (three times) for ionic measurement. The major water-soluble ions (WSIs, including Na^+, Mg^{2+}, K^+, Ca^{2+}, NH_4^+, Cl^-, NO_3^-, SO_4^{2-}) were detected by ion chromatography (Dionex ICS3000; Dionex Ltd., Sunnyvale, CA, USA) (Zhang et al., 2014). In this study, the WSI detection limit was 10 ng mL^{-1}, with an error of <5%. The $\delta^{15}N$ and $\delta^{18}O$ of NO_3^- were determined using a nitrous oxide (N_2O)-based isotopic procedure (McIlvin & Altabet, 2005; Tu et al., 2016). Briefly, NO_3^- (15 nmol L^{-1} in 5 mL solution) was initially reduced to nitrite (NO_2^-) by cadmium powder, and the intermediate NO_2^- was further reduced to N_2O using sodium azide in an acetic acid buffer (1:1 ratio of 20% acetic acid and sodium azide). Finally, the N and O isotopes in N_2O were analyzed using an isotope ratio mass spectrometer (MAT253; Thermo Fisher Scientific, Waltham, MA, USA). The $\delta^{15}N$–NO_3^- and $\delta^{18}O$–NO_3^- were expressed in parts per thousand according to standard guidelines (IAEA-NO-3, USGS32, USGS34, and USGS35):

$$\delta^{15}N = \left[\left(^{15}N/^{14}N\right)_{\text{sample}}/\left(^{15}N/^{14}N\right)_{\text{standard}} - 1\right] \times 1000$$

$$\delta^{18}O = \left[\left(^{18}O/^{16}O\right)_{\text{sample}}/\left(^{18}O/^{16}O\right)_{\text{standard}} - 1\right] \times 1000$$

The detailed processing steps have been reported in our previous study (Zong et al., 2017). Here, the analytical precision was <0.5‰ for $\delta^{15}N$–NO_3^- and 0.6‰ for $\delta^{18}O$–NO_3^-. Because the NO_2^- concentrations were mostly lower than the detection limit, and less than 0.3% of the NO_3^- detected, they were ignored during the isotopic analyses (Zong, Tian, et al., 2020). In addition, the concentrations of species in blank samples were all <3.1% of the average concentration for the total samples. It suggests that the samples collected were not contaminated during the processes, such as transportation and chemical analysis. For $PM_{2.5}$ and WSIs, their concentrations for each sample were recalculated by subtracting the average blank value. Of the 12 blank samples, 4 samples were below the detection line of isotopic measurement, and the remaining 8 samples averaged +1.9 ± 1.1‰ and +29.8 ± 28.2‰ for $\delta^{15}N$–NO_3^- and $\delta^{18}O$–NO_3^-, respectively. The isotope data (e.g., $\delta^{15}N$–NO_3^- and $\delta^{18}O$–NO_3^-) was then determined for each sample by mass balance (Zong, Tian, et al., 2020):

$$\delta^{15}N\text{-}NO_3^- = \frac{\delta^{15}N_{\text{sample}}\,[NO_3^-]_{\text{sample}} - \delta^{15}N_{\text{blank}}\,[NO_3^-]_{\text{blank}}}{[NO_3^-]_{\text{sample}} - [NO_3^-]_{\text{blank}}}$$

$$\delta^{18}O\text{-}NO_3^- = \frac{\delta^{18}O_{\text{sample}}\,[NO_3^-]_{\text{sample}} - \delta^{18}O_{\text{blank}}\,[NO_3^-]_{\text{blank}}}{[NO_3^-]_{\text{sample}} - [NO_3^-]_{\text{blank}}}$$

2.3. Bayesian Model

Bayesian model can estimate source contributions to a mixture, and shed light on the uncertainty associated with sources, fractionation, and isotopic signatures (Moore & Semmens, 2008). In its theorem, the contribution of each source can be assessed based on the mixed data and prior information:

$$P(f_q|x) = L(x|f_q) \times p(f_q) / \sum L(x|f_q) \times p(f_q)$$

where $L(x|f_q)$ is the likelihood of the proposed vectors (f_q) representing possible source contributions, and $p(f_q)$ refers to the prior probability of a given state of nature being true based on prior information (Parnell et al., 2013). To calculate the likelihood, source isotope distributions and their associated fractionation distributions are combined based on the assumption that the data are normally distributed and the f_i values comprising vector f_q are randomly generated:

$$\mu = \sum_{i=1}^{n} [f_i \times (\mu_i + \mu_\Delta)]$$

$$\sigma = \sqrt{\sum_{i=1}^{n} \left[f_i^2 \times (\sigma_i^2 + \sigma_\Delta^2)\right]}$$

where, μ_i and μ_Δ represent the mean value and mean fractionation of an isotope of the *i*th source, respectively, and σ_i and σ_Δ are the overall variance and variance in fractionation of an isotope of the *i*th source, respectively. Then the likelihood can be further expressed as:

$$L(x|\mu,\sigma) = \prod_{i=1}^{n} \left[\frac{1}{\sigma \times \sqrt{2\pi}} \times \exp\left(-\frac{(x_i - \mu)^2}{2\sigma^2}\right)\right]$$

where x_i is the ith isotopic value in the mixed data file. Based on the above principles, the Bayesian model has been widely used in quantitative studies of the sources of NO_3^-, especially after it was improved by incorporating the isotopic fractionation [ΔN ($\mu_\Delta \pm \sigma_\Delta$)] of the equilibrium/Leighton reaction in the conversion of NO_x to NO_3^-. For the isotopic fractionation (ΔN) between atmospheric $\delta^{15}N$–NO_3^- and $\delta^{15}N$–NO_x directly emitted by sources, please refer to Text S2, Table S3 in Supporting Information S1 and Zong et al. (2017) for details. According to the NO_x emission inventory and NO_3^- sources reported in North China, biomass burning (+0.3 ± 3.5‰), coal combustion (+13.7 ± 4.6‰), mobile sources including vehicle exhaust and ship emissions (−12.6 ± 2.2‰), and microbial processes (−33.8 ± 12.2‰) were considered to be end-members in the Bayesian simulations (Table S1 in Supporting Information S1) (Fan et al., 2020; Liu et al., 2017; Luo et al., 2019; Luo et al., 2021; Song et al., 2019; Zhang, Zheng, et al., 2020; Zong, Tian, et al., 2020).

2.4. Procedure for Analyzing the Evolution of NO_3^- Sources

The simulation results from Bayesian model represent the probability distribution of the contributions of various sources (Jin et al., 2021). However, the assessment of the multi-year evolution of different sources may be uncertain in this model because it is affected by the communal variation in different sources. For example, the contribution of coal combustion to NO_3^- may decrease when the contributions of other sources increase, but it is also possible that their emissions to NO_3^- concentration will all decrease over the long term. In this study, a method for tracing the evolutionary trend of NO_3^- sources was established, as follows:

$$\eta_{ij} = \frac{C_{ij}}{C_{ir}} = \frac{f_{ij} \times C_j}{f_{ir} \times C_r}$$

where η_{ij} is the rate of variation of source *i* in year *j* compared to the reference year, C_{ij} and C_{ir} refer to the distributing NO_3^- concentrations of source *i* in year *j* and the reference year, respectively. f_{ij} and C_j are the contribution of source *i* to the NO_3^- in year *j* (from Bayesian model), and the NO_3^- concentration in year *j*, respectively, and f_{ir} and C_r refer to the contributions of source *i* to the NO_3^- in the reference year, and the NO_3^- concentration in the reference year, respectively. Because the observation period was 2014–2019, 2014 was used as the reference year in this study.

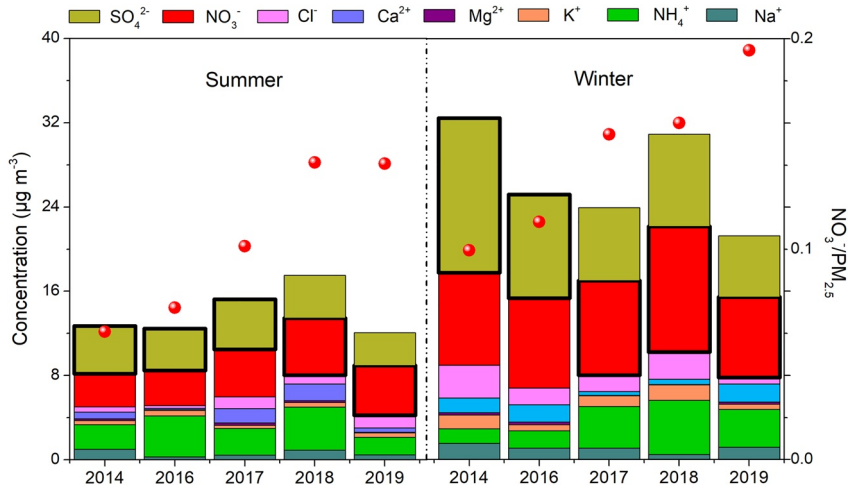

Figure 2. Variation of water-soluble ions (histogram, first y-axis) and the $NO_3^-/PM_{2.5}$ ratio (dot plot, secondary y-axis) in the atmosphere of Bohai Sea from 2014 to 2019. Bold outline indicates the greatest fraction of the water-soluble ions.

3. Results and Discussion

3.1. Overview of the $PM_{2.5}$ Concentration and Increasing NO_3^- Regime

Figure S2 in Supporting Information S1 shows the variation in $PM_{2.5}$ concentrations during the period 2014–2019. It is obvious that the $PM_{2.5}$ concentration observed was lower than that in the Beijing-Tianjin-Hebei region, reflecting the fact that the Bohai Sea is a background area of North China (Zong et al., 2018). The highest concentration was found in 2014 (61.6 ± 28.0 μg m^{-3}) and the lowest in 2019 (33.3 ± 12.9 μg m^{-3}), indicating a significant decline ($p < 0.01$). The decline confirms the effectiveness of China's particulate pollution control measures, although the measures need to be further strengthened based on the anomaly in 2018 (53.7 ± 29.0 μg m^{-3}) (Li, Gao, et al., 2021; Li, Ma, et al., 2021; Li, Wu, et al., 2021).

In $PM_{2.5}$, higher WSIs concentrations generally occurred in winter (Figure 2), and their proportions displayed an annual increase (Figure S3 in Supporting Information S1). WSIs contain important secondary inorganic components (i.e., SO_4^{2-}, NO_3^-, and NH_4^+). Although the concentrations of their precursors have been declining over time, the secondary components have not significantly decreased, which may be due to changes in reaction conditions, such as increasing levels of atmospheric oxidation (Fu et al., 2020). Furthermore, the composition of WSIs has undergone significant changes. Since 2014, SO_4^{2-} has been the most important component of WSIs in both summer and winter. However, as air pollution control in China has improved, the intensity of emission sources has changed greatly, especially coal combustion (Wang et al., 2020). In the winter of 2017, NO_3^- (15.0 ± 5.3%) surpassed SO_4^{2-} as the most important component, indicating that NO_3^- pollution in North China has become serious during the sampling period (Luo et al., 2021). This was confirmed by the observed variation of the $NO_3^-/PM_{2.5}$ ratio (Figure 2). From 2014 to 2019, the ratio displayed a significant upward trend in both winter (0.09–0.19) and summer (0.06–0.14) ($p < 0.01$), suggesting that control of NO_3^- is key to further reducing $PM_{2.5}$ concentration in North China (Text S3; Figure S4 in Supporting Information S1).

3.2. Formation and Sources of NO_3^- Inferred From Nitrogen and Oxygen Isotopes

The $\delta^{15}N$–NO_3^- values were distributed normally over a wide range (−4.1‰ to +20.5‰; Figure S5 in Supporting Information S1), with a mean value of +7.8 ± 5.0‰. Specially, the wintertime average $\delta^{15}N$–NO_3^- was +11.6 ± 4.3‰ (Figure 3), much higher than the summer value (+4.9 ± 3.2‰). According to the $\delta^{15}N$–NO_x distribution and the principle of isotope fractionation, the higher value in winter could be attributed to the increase in coal combustion seen during cold weather and enhancement of isotope fractionation. Based on the isotope fractionation theory (Walters & Michalski, 2015, 2016), the isotope fractionation caused by the temperature difference between summer and winter was 2.4‰, which is much lower than the observed divergence (~6.9‰). This suggests that the change in sources was the primary reason for the seasonal variation of $\delta^{15}N$–

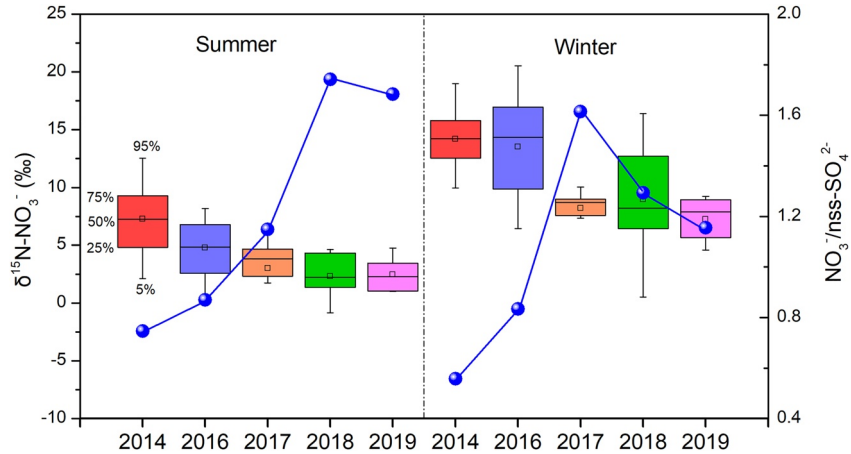

Figure 3. Characteristics of $\delta^{15}N\text{-}NO_3^-$ (box, first y-axis) and $NO_3^-/nss\text{-}SO_4^{2-}$ (line + dot, secondary y-axis) in the Bohai Sea from 2014 to 2019.

NO_3^- (Zhao et al., 2020; Zong, Tan, et al., 2020). From 2014 to 2019 (except for winter 2018 and summer 2019), the $\delta^{15}N\text{–}NO_3^-$ in summer displayed a relatively steady downward trend, while the decrease in winter was more intense, especially in the winter of 2017. It indicates a decline in the amount of coal consumption, consistent with the reported changes in China's energy use (Figure S6 in Supporting Information S1) (Lu et al., 2020). While the sharp decline in the winter of 2017 compared to that of 2016 was consistent with China's residential coal use control policies at that time (Wang et al., 2020). Beginning in October 2016, the Ministry of Chinese Environmental Protection issued "Technical Guidelines for the Comprehensive Treatment of Civil Coal Combustion Pollution" and "Technical Guidelines for the Compilation of Civil Coal Air Pollutant Emission Inventories," with the aim of reducing emissions from residential coal combustion. The observed sharp decline demonstrates the effectiveness of these pollution control policies, but the anomaly in the winter of 2018 indicates that greater adherence is still required. The $NO_3^-/nss\text{-}SO_4^{2-}$ ratio could reflect the ratio between mobile sources (e.g., vehicle exhaust) and stationary sources (e.g., coal combustion) (Itahashi et al., 2018; Zong et al., 2016). The annual variation of this ratio showed an overall upward trend with a few anomalies, indicating a decrease in coal combustion and an increase in the proportion of mobile sources. Especially in summer, a continuous increase was seen in the contribution of mobile sources in China, including vehicle exhaust and shipping emissions, to NO_x (Zhang et al., 2018). The volatility in winter also reflects uncertainty in the effectiveness of controls on residential coal emissions.

The average value of $\delta^{18}O\text{–}NO_3^-$ was +72.6 ± 13.5‰ (range: +31.3‰ to +100.0‰; Figure 4), which was well within the broad range of values previously reported (Fang et al., 2011; Michalski et al., 2012). Generally, the formation pathways of NO_3^- in the atmosphere are relatively complicated (R_1–R_{12}), but the main ones are the O_3 and •OH pathways (Zong et al., 2017). Studies have shown that the processes of NO converting into NO_2 through HO_2 or ROO (R_4–R_5) and the HC pathway (R_8, generally <5%) are limited (Alexander et al., 2020; Xiao et al., 2020), so they were ignored in this study. From 2014 to 2019, $\delta^{18}O\text{–}NO_3^-$ oscillated in summer, with increases seen in winter. This indicates an increase in the contribution of the O_3 pathway to the formation of NO_3^-, consistent with the increasingly serious O_3 pollution seen in this region (Li, Jacob, Liao, Zhu, et al., 2019). In the atmosphere, the oxygen atoms of NO_x are rapidly exchanged with O_3 in the NO/NO_2 cycle (R_1–R_3), then the balanced NO_x mainly reacts with •OH or O_3 to form HNO_3 (R_6–R_7, R_9–R_{11}), which is further converted to NO_3^- on alkaline surfaces (R_{12}) (Hastings et al., 2003). Therefore, it is assumed that two-thirds of the oxygen atoms in NO_3^- are derived from O_3 and one-third from •OH in the •OH generation pathway; correspondingly, five-sixths of the oxygen atoms are derived from O_3 and one-sixth from •OH in the O_3 pathway. Based on the ranges of $\delta^{18}O\text{–}O_3$ (90 ~ 122‰) and $\delta^{18}O\text{–}H_2O$ (−25 ~ 0‰) values (Fang et al., 2011), the respective contributions of the two generation pathways were assessed by a Monte Carlo simulation (Zong et al., 2017), and the range and median of the contribution for the •OH generation pathway are shown in Figure 4. The average contributions of the •OH pathway in summer and winter were 61.8 ± 18.3% and 36.3 ± 20.6%, respectively. This indicates a transition of the dominant pathway of NO_3^- formation from the •OH pathway in summer to the O_3 pathway in winter (Xiao et al., 2020). The contribution of the •OH pathway was largest in the summer of 2017 (73.56 ± 13.24%),

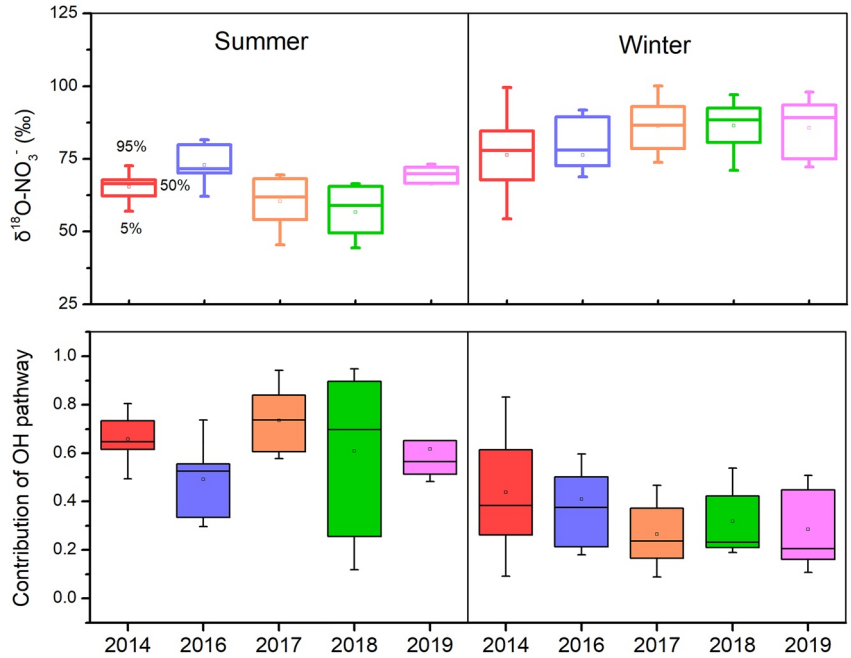

Figure 4. Characteristics of $\delta^{18}O–NO_3^-$ and the corresponding contribution of •OH pathway in the formation of NO_3^-.

and smallest in the winter of 2017 (26.54 ± 13.63%). The highest value and the lowest value both appeared in this year, indicating a substantial change in the dominant species of atmospheric oxidants (e.g., •OH and O_3). The main direct sources of O_3 or •OH are volatile organic compounds (VOCs) and NO_x; therefore, the changes in the levels of oxidants may have been caused by the variation of emission sources in 2017, which was consistent with the change of $\delta^{15}N–NO_3^-$ with a sharp decline in the winter (Figure 3) (Tao et al., 2018). Compared to 2014, the contribution of the •OH pathway declined by 6.4% and 27.4% in the summer and winter of 2019, respectively, further indicating that O_3 pollution in North China has increased.

$$NO + O_3 \rightarrow NO_2 + O_2 \quad \text{(R1)}$$

$$NO_2 + hv \rightarrow NO + O \quad \text{(R2)}$$

$$O + O_2 \rightarrow O_3 \quad \text{(R3)}$$

$$H\,(\text{or } R) + O_2 \rightarrow HO_2\,(\text{or ROO}) \quad \text{(R4)}$$

$$NO + HO_2\,(\text{or ROO}) \rightarrow NO_2 + \bullet OH\,(\text{or RO}\bullet) \quad \text{(R5)}$$

$$NO_2 + \bullet OH + M \rightarrow HNO_3 + M \quad \text{(R6)}$$

$$NO_2 + O_3 \rightarrow NO_3 + O_2 \quad \text{(R7)}$$

$$NO_3 + HC \rightarrow HNO_3 + R \quad \text{(R8)}$$

$$NO_2 + NO_3 \leftarrow \rightarrow N_2O_5 \quad \text{(R9)}$$

$$N_2O_5 + H_2O + \text{surface} \rightarrow 2HNO_3 \quad \text{(R10)}$$

$$N_2O_5 + H_2O(g) \rightarrow 2HNO_3 \quad \text{(R11)}$$

$$HNO_3 + \text{alkaline surface} \rightarrow NO_3^- \quad \text{(R12)}$$

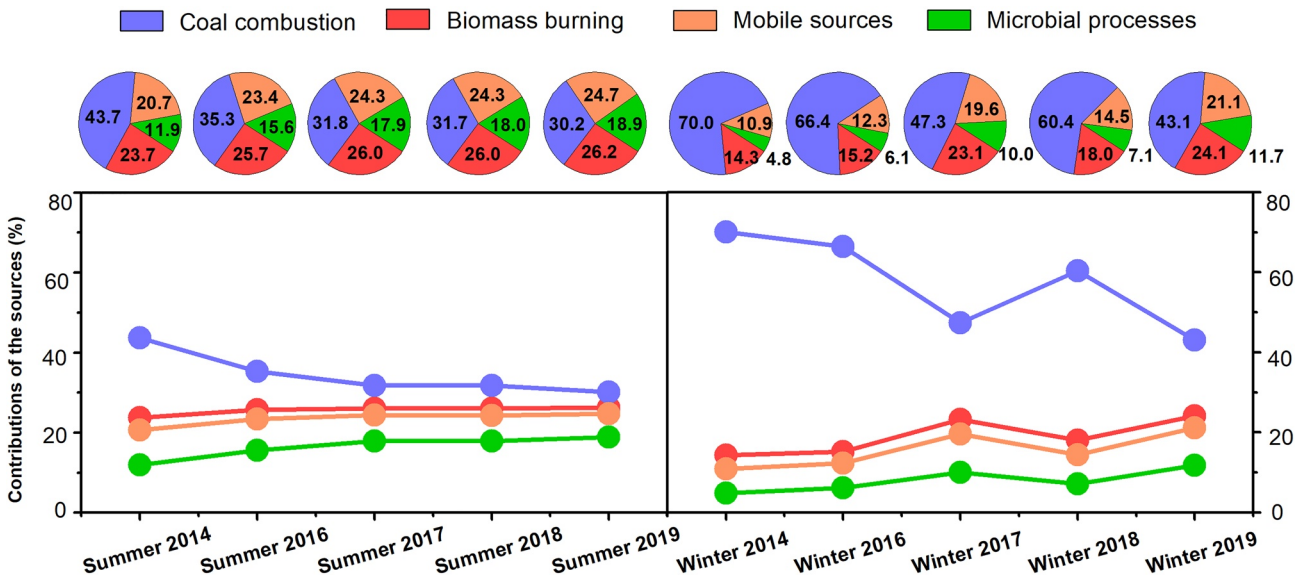

Figure 5. Multi-year variation of NO_3^- sources (biomass burning, coal combustion, mobile sources, and microbial processes) inferred from the Bayesian model (the value expressed in the figure represents the average values in the distribution of the contributions).

3.3. Source Apportionment of NO_3^- Based on the Bayesian Model

To further explore the source variations of NO_3^-, Bayesian simulations of overall, annual, and seasonal patterns were conducted in this study. Results show that the average contributions of biomass burning, coal combustion, mobile sources, and microbial processes were 22.1 ± 5.8%, 46.6 ± 15.9%, 19.4 ± 6.2%, and 11.9 ± 6.0%, respectively, in the two seasons from 2014 to 2019 (Table S4 in Supporting Information S1). These proportions indicate that coal combustion was still the primary source of NO_3^- in North China, especially in winter (59.3 ± 14.2%) (Fan et al., 2020). However, the dominance of coal combustion as a source of NO_3^- progressively decreased over the study period (Figure 5). In 2019, the contributions of coal combustion were 30.2% and 43.1% in summer and winter, representing decreases of 13.5% and 26.9% compared to 2014, respectively. Coal consumption can be roughly divided into industrial and civilian uses, with the latter mostly occurring in winter (i.e., for heating), especially in North China (Liu et al., 2016). Therefore, the greater reduction of coal combustion in winter may be attributed to the control of dispersed coal as a fuel source (Liang et al., 2021). If the decrease in summer can be regarded as part of the conventional decreasing trend in coal consumption (Figure S6 in Supporting Information S1), then the decrease due to control of residential use in winter was 13.4%. This coincided with the ~14% reduction in the $PM_{2.5}$ concentration reported by a recent study in association with dispersed coal management (Wang et al., 2020). In 2017, the Beijing-Tianjin-Hebei region and surrounding areas completed a replacement program, of coal to gas and electricity, in nearly 6 million households. Among them, 4.75 million households were in one of the "2 + 26" pilot cities, and a "no burning" area for dispersed coal about 10,000 km^2 in extent was designated. As a result, it is estimated that about 18 million tons of coal burning has been avoided, with 70% being replaced by natural gas (Yan et al., 2020). However, this project still faces several difficulties: a clean energy supply (e.g., gas and electricity) is lacking in winter; the cost of renewable energy heating remains relatively high; and management of dispersed coal is still overly dependent on government subsidies, given the financial demands. Under the influence of these constraints, reburning of dispersed coal has occasionally occurred in North China, and differences in regional policies can also cause "pollution leakage." While a relatively smooth and gradual downward trend of the contribution of coal combustion to NO_3^- was seen in summer from 2014 to 2019, in winter there was a major anomaly in the winter of 2018, which reflected the reburning of dispersed coal. Overall, the "coal replacement" program in North China has played a very positive role in the management of $PM_{2.5}$ and NO_3^- pollution, but more policies and technologies need to be developed to promote its implementation (Zhao et al., 2018).

The contributions of the other three sources of NO_3^- were higher in summer than in winter, suggesting that the emission intensities of these sources were relatively high in summer. Generally, the microbial processes that produce NO_x refer to the nitrification and denitrification, which mainly occur in soil and are affected by temper-

ature (Su et al., 2020). The summer season in North China is hot and wet, where the temperature and humidity are conducive to these microbial activities (Yu et al., 2021). Furthermore, North China has a large area of cultivated land, resulting that NO_x emissions from microbial processes are intensive, especially after the fertilization in spring (Tian et al., 2017). In addition, multiple studies have shown that biomass burning in summer is a very important source of emissions, which is also in accordance with its large contribution in this study (Wang et al., 2014). During the 2014–2019 period, the contributions of these sources all displayed an upward trend in both summer and winter, in line with the changing characteristics of these sources. The increasing contributions of biomass burning and microbial processes may be related to the continuous expansion of cultivated land in North China. Although there is no direct data for North China, the area of cultivated land in China increased from 6.5×10^7 ha in 2014 to 6.9×10^7 ha in 2019. It increased the production of biomass wastes and the use of fertilizers in turn. For example, the amount of compound fertilizer used has increased by 1.2 million tons from 2014 to 2019. As mentioned above, microbial processes in soil are important sources of NO_x, especially after fertilization; the increase of biomass waste would inevitably lead to the increase of NO_x from biomass burning (Su et al., 2011; Zong et al., 2016). These factors have contributed to the growth in contributions from the two sources. According to the China Vehicle Environmental Management Annual Report, the average annual growth rate of car ownership has exceeded 10% since 2011, and the total number of vehicles on the road reached 348 million in 2020. Furthermore, the increase in the contribution of mobile sources is also related to the increase in shipping emissions in the Bohai Sea (Zhang et al., 2018). For example, the container throughput of Tianjin Port in 2020 reached 18.4 million twenty-foot equivalent units, a year-on-year increase of 6.1%, indicating an increase in shipping activities and, by extension, emissions. In addition, the increase of mobile sources was consistent with the variation of NO_3^-/nss-SO_4^{2-} ratio discussed above.

3.4. Driving Factors of the Aggravation of NO_3^- Pollution in North China

For exploring the evolutionary characteristics of NO_3^- sources, the NO_3^- concentrations were reanalyzed according to the Bayesian results. Annual variation (η) was determined based on the reference value (2014). Surprisingly, there was a trend toward an annual increase in summer values for coal combustion (Figure 6), contrary to the general decrease in emission intensity confirmed above (Lu et al., 2020). This can be ascribed to the increase in the rate of conversion from NO_x to NO_3^-. Following unprecedented campaigns to improve air quality in China, the average NO_x concentration has decreased (Liu et al., 2017). This is most apparent in the Bohai Sea, where the NO_2 concentration decreased from 38.8 ± 12.4 μg m^{-3} in 2014 to 27.7 ± 12.3 μg m^{-3} in 2019. However, due to changes in conversion conditions, especially increase in atmospheric oxidation (Li, Jacob, Liao, Shen, et al., 2019), the NO_x conversion rate has increased (Figure S7 in Supporting Information S1). For example, the

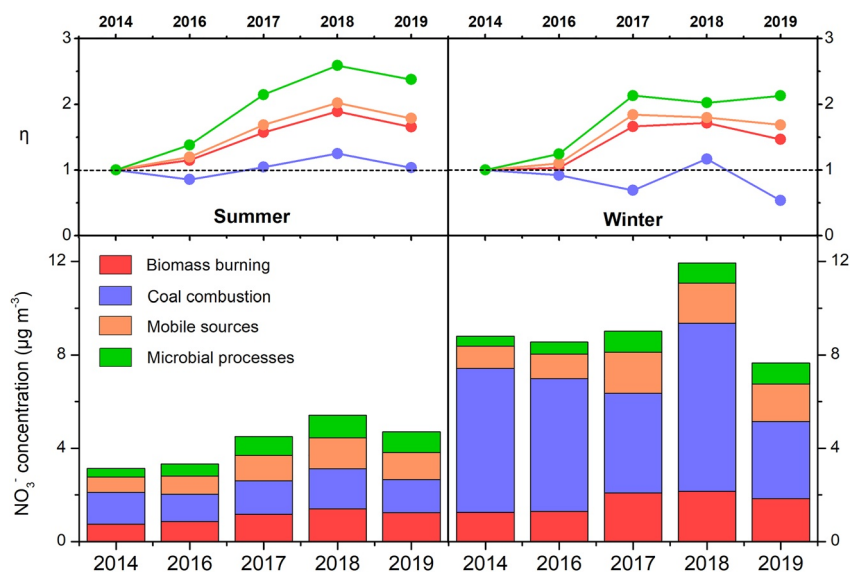

Figure 6. Redistribution and annual variation (from 2014 to 2019) of NO_3^- based on the Bayesian model results. The reference year for ratio calculations was 2014.

nitrogen oxidation ratio, defined as the molar ratio of NO_3^- to NO_3^- + NO_x, was 0.03 in the summer of 2014, while it reached 0.07 in the summer of 2019. This growth is consistent with the increase in O_3 concentration in the Bohai Sea, which increased from 84.5 ± 48.6 μg m^{-3} in 2014 to 98.6 ± 42.9 μg m^{-3} in 2019. In addition, $\delta^{18}O$–NO_3^- from 2014 to 2019 oscillated in summer, with increases seen in winter (Figure 4). This indicates the increase in atmospheric oxidation in North China may be mainly caused by O_3 pollution (Li, Jacob, Liao, Shen, et al., 2019; Zhang et al., 2021). Compared to 2014, the contribution of the •OH pathway in NO_3^- formation declined by 6.4% and 27.4% in the summer and winter of 2019, respectively, further consistent with the increasingly serious O_3 pollution seen in this region. There is an urgent need to manage this situation, and a similar conclusion for the persistent heavy nitrate pollution in Northern China was also proposed by Fu et al. (2020) based on CMAQ simulation.

As for other sources, biomass burning and mobile sources made similar contributions to atmospheric NO_3^-, with a relatively consistent upward trend over the study period. However, the contribution of microbial processes to the NO_3^- concentration increased even more. For example, the concentrations of NO_3^- contributed by microbial processes were 0.37 μg m^{-3} and 0.42 μg m^{-3}, respectively, in the summer and winter of 2014; while they increased to 0.89 μg m^{-3} and 0.90 μg m^{-3}, in 2019 with the η reaching 2.4 and 2.1, respectively (Figure 6). The η values were much higher than those of biomass burning (summer: 1.6; winter: 1.5) and mobile sources (summer: 1.8; winter 1.7), respectively. Microbial processes are typically neglected in air quality models and emission control strategy assessments in North China (Lu et al., 2021), however, our results indicate that more attention needs to be given to them. Wang et al. (2007) shows that the microbial source of NO_x peaked in summer, accounting for as much as 43% of the combustion sources, while it was not important in winter. However, Fan et al. (2020) finds that the contribution of microbial processes to NO_x increased significantly during the winter haze in Beijing, which could be doubled compared with the clean period. All these evidences illustrate the increasing importance of microbial processes to air pollution. As mentioned above, microbial processes mainly occur in soil, and the most important artificial source to control is nitrogen fertilizer (Liu et al., 2021). In fact, a huge amount of nitrogen fertilizer is used in the North China Plain, which is thus an important source of microbial pollution in China (Zong, Tan, et al., 2020). Especially, the use of a large amount of nitrogen fertilizer during the cultivation period could significantly increase the amounts of NO_3^- precursors (e.g., NO_x, O_3) (Lu et al., 2021). Therefore, reasonable levels of fertilization during cultivation, and replacement of artificial fertilizers with more suitable organic ones, will be beneficial for alleviating the NO_3^- pollution in this region. Overall, NO_3^- pollution in the Bohai Sea and North China is increasing. To ensure effective pollution control, there needs to be greater focus on the control of O_3 pollution; more comprehensive policies to reduce the emissions of VOCs, NO_x, and other precursors of O_3 are needed (Yuan et al., 2013). More attention should be focused on microbial processes, which have been largely neglected (Lu et al., 2021), in addition to the strict governance of significant emission sources (e.g., residential coal combustion).

4. Conclusion

Exploring the evolution of atmospheric NO_3^- is the key to further mitigating $PM_{2.5}$ pollution in North China. In this study, multi-year offshore observations were conducted in the Bohai Sea, and the sources and formation of NO_3^- were apportioned based on the isotope technique and Bayesian model. Results show that the proportion of NO_3^- in $PM_{2.5}$ increased significantly from 2014 (0.08) to 2019 (0.16), suggesting the increasing contribution of NO_3^- to $PM_{2.5}$ pollution in North China. Bayesian simulation indicates that coal combustion was the most important source of NO_3^- (46.6 ± 15.9%), but it has displayed a significant inter-annual decline. The decline was consistent with the control of wintertime coal emissions in North China; however, a rebound in 2018 indicates the need for sustaining the coal control efforts. The ratio of NO_3^- formed through the O_3 pathway has increased greatly, especially in the winter. Therefore, our results suggest that the increase in O_3 concentration could lead to an increase in atmospheric oxidation, thereby boosting the conversion rate of NO_x to NO_3^-. This increase can even offset China's efforts to reduce NO_x emissions. Unexpectedly, the contribution of microbial processes has increased significantly. It indicates that the source, which is often overlooked, needs to be incorporated into future control measures. Overall, this study emphasizes the key roles of atmospheric oxidation and microbial processes in aggravating NO_3^- pollution. Our results provide useful reference to alleviate the increasingly serious NO_3^- pollution, and thereby further reduce the $PM_{2.5}$ concentration in North China.

Data Availability Statement

The data used in this study is available at: Zong et al. (2022), Data set of nitrate in North China: Isotopic information from 10 offshore cruises in the Bohai Sea from 2014 to 2019 [Dataset], Zenodo, https://doi.org/10.5281/zenodo.6420620.

Acknowledgments
This research was financially supported by the Natural Scientific Foundation of China (NSFC; Grant Nos: 41907198, 41977190), the NSFC-Shandong Joint Fund (U1906215). Additional support to Z.Z. and T.W. was provided by the Hong Kong Research Grants Council (project no. T24-504/17-N). This research was also very grateful for the sampling support of RV CHUANGXINYI and the data sources (NO_2 and O_3, https://www.aqistudy.cn/historydata/).

References

Alexander, B., Sherwen, T., Holmes, C. D., Fisher, J. A., Chen, Q., Evans, M. J., & Kasibhatla, P. (2020). Global inorganic nitrate production mechanisms: Comparison of a global model with nitrate isotope observations. *Atmospheric Chemistry and Physics*, *20*(6), 3859–3877. https://doi.org/10.5194/acp-20-3859-2020

Fan, M. Y., Zhang, Y. L., Lin, Y. C., Cao, F., Zhao, Z. Y., Sun, Y., et al. (2020). Changes of emission sources to nitrate aerosols in Beijing after the clean air actions: Evidence from dual isotope compositions. *Journal of Geophysical Research: Atmospheres*, *125*(12), e2019JD031998. https://doi.org/10.1029/2019jd031998

Fang, Y. T., Koba, K., Wang, X. M., Wen, D. Z., Li, J., Takebayashi, Y., et al. (2011). Anthropogenic imprints on nitrogen and oxygen isotopic composition of precipitation nitrate in a nitrogen-polluted city in southern China. *Atmospheric Chemistry and Physics*, *11*(3), 1313–1325. https://doi.org/10.5194/acp-11-1313-2011

Fu, X., Wang, T., Gao, J., Wang, P., Liu, Y., Wang, S., et al. (2020). Persistent heavy winter nitrate pollution driven by increased photochemical oxidants in northern China. *Environmental Science & Technology*, *54*(7), 3881–3889. https://doi.org/10.1021/acs.est.9b07248

Gu, M., Pan, Y., Walters, W. W., Sun, Q., Song, L., Wang, Y., et al. (2022). Vehicular emissions enhanced ammonia concentrations in winter mornings: Insights from diurnal nitrogen isotopic signatures. *Environmental Science & Technology*, *56*(3), 1578–1585. https://doi.org/10.1021/acs.est.1c05884

Hastings, M. G., Sigman, D. M., & Lipschultz, F. (2003). Isotopic evidence for source changes of nitrate in rain at Bermuda. *Journal of Geophysical Research*, *108*(D24), 4790–4812. https://doi.org/10.1029/2003jd003789

Itahashi, S., Yumimoto, K., Uno, I., Hayami, H., Fujita, S.-i., Pan, Y., & Wang, Y. (2018). A 15-year record (2001–2015) of the ratio of nitrate to non-sea-salt sulfate in precipitation over East Asia. *Atmospheric Chemistry and Physics*, *18*(4), 2835–2852. https://doi.org/10.5194/acp-18-2835-2018

Jin, Z., Qian, L., Shi, Y., Fu, G., Li, G., & Li, F. (2021). Quantifying major NO_x sources of aerosol nitrate in Hangzhou, China, by using stable isotopes and a Bayesian isotope mixing model. *Atmospheric Environment*, *244*, 117979. https://doi.org/10.1016/j.atmosenv.2020.117979

Li, H., Ma, Y., Duan, F., Zhu, L., Ma, T., Yang, S., et al. (2021). Stronger secondary pollution processes despite decrease in gaseous precursors: A comparative analysis of summer 2020 and 2019 in Beijing. *Environmental Pollution*, *279*, 116923. https://doi.org/10.1016/j.envpol.2021.116923

Li, J., Gao, W., Cao, L., Xiao, Y., Zhang, Y., Zhao, S., et al. (2021). Significant changes in autumn and winter aerosol composition and sources in Beijing from 2012 to 2018: Effects of clean air actions. *Environmental Pollution*, *268*(Pt B), 115855. https://doi.org/10.1016/j.envpol.2020.115855

Li, J., Wu, Y., Ren, L., Wang, W., Tao, J., Gao, Y., et al. (2021). Variation in $PM_{2.5}$ sources in central North China Plain during 2017–2019: Response to mitigation strategies. *Journal of Environmental Management*, *288*, 112370. https://doi.org/10.1016/j.jenvman.2021.112370

Li, K., Jacob, D. J., Liao, H., Shen, L., Zhang, Q., & Bates, K. H. (2019). Anthropogenic drivers of 2013–2017 trends in summer surface ozone in China. *Proceedings of the National Academy of Sciences of the United States of America*, *116*(2), 422–427. https://doi.org/10.1073/pnas.1812168116

Li, K., Jacob, D. J., Liao, H., Zhu, J., Shah, V., Shen, L., et al. (2019). A two-pollutant strategy for improving ozone and particulate air quality in China. *Nature Geoscience*, *12*(11), 906–910. https://doi.org/10.1038/s41561-019-0464-x

Liang, J., He, P., & Qiu, Y. (2021). Energy transition, public expressions, and local officials? incentives: Social media evidence from the coal-to-gas transition in China. *Journal of Cleaner Production*, *298*, 126771. https://doi.org/10.1016/j.jclepro.2021.126771

Liu, F., Beirle, S., Zhang, Q., van Der, A. R., Zheng, B., Tong, D., & He, K. (2017). NO_x emission trends over Chinese cities estimated from OMI observations during 2005 to 2015. *Atmospheric Chemistry and Physics*, *17*(15), 9261–9275. https://doi.org/10.5194/acp-17-9261-2017

Liu, J., Mauzerall, D. L., Chen, Q., Zhang, Q., Song, Y., Peng, W., et al. (2016). Air pollutant emissions from Chinese households: A major and underappreciated ambient pollution source. *Proceedings of the National Academy of Sciences of the United States of America*, *113*(28), 7756–7761. https://doi.org/10.1073/pnas.1604537113

Liu, Y., Lin, B., & Xu, B. (2021). Modeling the impact of energy abundance on economic growth and CO_2 emissions by quantile regression: Evidence from China. *Energy*, *227*, 120416. https://doi.org/10.1016/j.energy.2021.120416

Lu, X., Ye, X., Zhou, M., Zhao, Y., Weng, H., Kong, H., et al. (2021). The underappreciated role of agricultural soil nitrogen oxide emissions in ozone pollution regulation in North China. *Nature Communications*, *12*(1), 5021. https://doi.org/10.1038/s41467-021-25147-9

Lu, X., Yuan, D., Chen, Y., Fung, J. C. H., Li, W., & Lau, A. K. H. (2020). Estimations of Long-Term nss-SO_4^{2-} and NO_3^- Wet Depositions over East Asia by Use of Ensemble Machine-Learning Method. *Environmental Science & Technology*, *54*(18), 11118–11126. https://doi.org/10.1021/acs.est.0c01068

Luo, L., Kao, S.-J., Bao, H., Xiao, H., Xiao, H., Yao, X., et al. (2018). Sources of reactive nitrogen in marine aerosol over the Northwest Pacific Ocean in spring. *Atmospheric Chemistry and Physics*, *18*(9), 6207–6222. https://doi.org/10.5194/acp-18-6207-2018

Luo, L., Wu, Y., Xiao, H., Zhang, R., Lin, H., Zhang, X., & Kao, S.-J. (2019). Origins of aerosol nitrate in Beijing during late winter through spring. *The Science of the Total Environment*, *653*, 776–782. https://doi.org/10.1016/j.scitotenv.2018.10.306

Luo, L., Zhu, R. G., Song, C. B., Peng, J. F., Guo, W., Liu, Y., et al. (2021). Changes in nitrate accumulation mechanisms as $PM_{2.5}$ levels increase on the North China Plain: A perspective from the dual isotopic compositions of nitrate. *Chemosphere*, *263*, 127915. https://doi.org/10.1016/j.chemosphere.2020.127915

McIlvin, M. R., & Altabet, M. A. (2005). Chemical conversion of nitrate and nitrite to nitrous oxide for nitrogen and oxygen isotopic analysis in freshwater and seawater. *Analytical Chemistry*, *77*(17), 5589–5595. https://doi.org/10.1021/ac050528s

Michalski, G., Bhattacharya, S. K., & Mase, D. F. (2012). Oxygen isotope dynamics of atmospheric nitrate and its precursor molecules. *Handbook of Environmental Isotope Geochemistry*, *II*, 613–638. https://doi.org/10.1007/978-3-642-10637-8_30

Moore, J. W., & Semmens, B. X. (2008). Incorporating uncertainty and prior information into stable isotope mixing models. *Ecology Letters*, *11*(5), 470–480. https://doi.org/10.1111/j.1461-0248.2008.01163.x

Parnell, A. C., Phillips, D. L., Bearhop, S., Semmens, B. X., Ward, E. J., Moore, J. W., et al. (2013). Bayesian stable isotope mixing models. *Environmetrics*, *24*(6), 387–399. https://doi.org/10.1002/env.2221

Peng, J., Hu, M., Shang, D., Wu, Z., Du, Z., Tan, T., et al. (2021). Explosive secondary aerosol formation during severe haze in the North China Plain. *Environmental Science & Technology*, *55*(4), 2189–2207. https://doi.org/10.1021/acs.est.0c07204

Song, W., Wang, Y. L., Yang, W., Sun, X. C., Tong, Y. D., Wang, X. M., et al. (2019). Isotopic evaluation on relative contributions of major NO_x sources to nitrate of $PM_{2.5}$ in Beijing. *Environmental Pollution*, *248*, 183–190. https://doi.org/10.1016/j.envpol.2019.01.081

Su, C., Kang, R., Zhu, W., Huang, W., Song, L., Wang, A., et al. (2020). Delta N-15 of Nitric Oxide Produced Under Aerobic or Anaerobic Conditions From Seven Soils and Their Associated N Isotope Fractionations. *Journal of Geophysical Research-Biogeosciences*, *125*(9), e2020JG005705. https://doi.org/10.1029/2020jg005705

Su, H., Cheng, Y., Oswald, R., Behrendt, T., Trebs, I., Meixner, F. X., et al. (2011). Soil nitrite as a source of atmospheric HONO and OH radicals. *Science*, *333*(6049), 1616–1618. https://doi.org/10.1126/science.1207687

Tao, S., Ru, M. Y., Du, W., Zhu, X., Zhong, Q. R., Li, B. G., et al. (2018). Quantifying the rural residential energy transition in China from 1992 to 2012 through a representative national survey. *Nature Energy*, *3*(7), 567–573. https://doi.org/10.1038/s41560-018-0158-4

Tian, D., Zhang, Y., Zhou, Y., Mu, Y., Liu, J., Zhang, C., & Liu, P. (2017). Effect of nitrification inhibitors on mitigating N_2O and NO emissions from an agricultural field under drip fertigation in the North China Plain. *The Science of the Total Environment*, *598*, 87–96. https://doi.org/10.1016/j.scitotenv.2017.03.220

Tu, Y., Fang, Y., Liu, D., & Pan, Y. (2016). Modifications to the azide method for nitrate isotope analysis. *Rapid Communications in Mass Spectrometry*, *30*(10), 1213–1222. https://doi.org/10.1002/rcm.7551

Walters, W. W., & Michalski, G. (2015). Theoretical calculation of nitrogen isotope equilibrium exchange fractionation factors for various NO_y molecules. *Geochimica et Cosmochimica Acta*, *164*, 284–297. https://doi.org/10.1016/j.gca.2015.05.029

Walters, W. W., & Michalski, G. (2016). Theoretical calculation of oxygen equilibrium isotope fractionation factors involving various NO_y molecules, OH, and H_2O and its implications for isotope variations in atmospheric nitrate. *Geochimica et Cosmochimica Acta*, *191*, 89–101. https://doi.org/10.1016/j.gca.2016.06.039

Wang, S., Su, H., Chen, C., Tao, W., Streets, D. G., Lu, Z., et al. (2020). Natural gas shortages during the "coal-to-gas" transition in China have caused a large redistribution of air pollution in winter 2017. *Proceedings of the National Academy of Sciences of the United States of America*, *117*(49), 31018–31025. https://doi.org/10.1073/pnas.2007513117

Wang, X., Chen, Y., Tian, C., Huang, G., Fang, Y., Zhang, F., et al. (2014). Impact of agricultural waste burning in the Shandong Peninsula on carbonaceous aerosols in the Bohai Rim, China. *The Science of the Total Environment*, *481*, 311–316. https://doi.org/10.1016/j.scitotenv.2014.02.064

Wang, Y., McElroy, M. B., Martin, R. V., Streets, D. G., Zhang, Q., & Fu, T.-M. (2007). Seasonal variability of NO_x emissions over east China constrained by satellite observations: Implications for combustion and microbial sources. *Journal of Geophysical Research*, *112*(D6), D06301. https://doi.org/10.1029/2006jd007538

Xiao, H. W., Zhu, R. G., Pan, Y. Y., Guo, W., Zheng, N. J., Liu, Y. H., et al. (2020). Differentiation between nitrate aerosol formation pathways in a southeast Chinese city by dual isotope and modeling studies. *Journal of Geophysical Research: Atmospheres*, *125*(13), e2020JD032604. https://doi.org/10.1029/2020jd032604

Xu, Q., Wang, S., Jiang, J., Bhattarai, N., Li, X., Chang, X., et al. (2019). Nitrate dominates the chemical composition of $PM_{2.5}$ during haze event in Beijing, China. *The Science of the Total Environment*, *689*, 1293–1303. https://doi.org/10.1016/j.scitotenv.2019.06.294

Yan, Y., Jiao, W., Wang, K., Huang, Y., Chen, J., & Han, Q. (2020). Coal-to-gas heating compensation standard and willingness to make clean energy choices in typical rural areas of northern China. *Energy Policy*, *145*, 111698. https://doi.org/10.1016/j.enpol.2020.111698

Yang, Y., Wang, Y., Huang, W., Yao, D., Zhao, S., Wang, Y., et al. (2021). Parameterized atmospheric oxidation capacity and speciated OH reactivity over a suburban site in the North China Plain: A comparative study between summer and winter. *The Science of the Total Environment*, *773*, 145264. https://doi.org/10.1016/j.scitotenv.2021.145264

Yu, J., Zhang, W., Tan, Y., Zong, Z., Hao, Q., Tian, C., et al. (2021). Dual-isotope-based source apportionment of nitrate in 30 rivers draining into the Bohai Sea, north China. *Environmental Pollution*, *283*, 117112. https://doi.org/10.1016/j.envpol.2021.117112

Yuan, B., Hu, W. W., Shao, M., Wang, M., Chen, W. T., Lu, S. H., et al. (2013). VOC emissions, evolutions and contributions to SOA formation at a receptor site in eastern China. *Atmospheric Chemistry and Physics*, *13*(17), 8815–8832. https://doi.org/10.5194/acp-13-8815-2013

Zhai, S., Jacob, D. J., Wang, X., Liu, Z., Wen, T., Shah, V., et al. (2021). Control of particulate nitrate air pollution in China. *Nature Geoscience*, *14*(6), 389–395. https://doi.org/10.1038/s41561-021-00726-z

Zhang, F., Chen, Y., Chen, Q., Feng, Y., Shang, Y., Yang, X., et al. (2018). Real-world emission factors of gaseous and particulate pollutants from marine fishing boats and their total emissions in China. *Environmental Science & Technology*, *52*(8), 4910–4919. https://doi.org/10.1021/acs.est.7b04002

Zhang, F., Chen, Y., Tian, C., Wang, X., Huang, G., Fang, Y., & Zong, Z. (2014). Identification and quantification of shipping emissions in Bohai Rim, China. *The Science of the Total Environment*, *497–498*, 570–577. https://doi.org/10.1016/j.scitotenv.2014.08.016

Zhang, Q., & Geng, G. (2019). Impact of clean air action on $PM_{2.5}$ pollution in China. *Science China Earth Sciences*, *62*(12), 1845–1846. https://doi.org/10.1007/s11430-019-9531-4

Zhang, Y., Xue, L., Li, H., Chen, T., Mu, J., Dong, C., et al. (2021). Source apportionment of regional ozone pollution observed at Mount Tai, North China: Application of Lagrangian photochemical trajectory model and implications for control policy. *Journal of Geophysical Research: Atmospheres*, *126*(6). https://doi.org/10.1029/2020jd033519

Zhang, Z., Guan, H., Luo, L., Zheng, N., Xiao, H., Liang, Y., & Xiao, H. (2020). Sources and transformation of nitrate aerosol in winter 2017–2018 of megacity Beijing: Insights from an alternative approach. *Atmospheric Environment*, *241*, 117842. https://doi.org/10.1016/j.atmosenv.2020.117842

Zhang, Z., Zheng, N., Zhang, D., Xiao, H., Cao, Y., & Xiao, H. (2020). Rayleigh based concept to track NO_x emission sources in urban areas of China. *The Science of the Total Environment*, *704*, 135362. https://doi.org/10.1016/j.scitotenv.2019.135362

Zhao, B., Zheng, H., Wang, S., Smith, K. R., Lu, X., Aunan, K., et al. (2018). Change in household fuels dominates the decrease in $PM_{2.5}$ exposure and premature mortality in China in 2005–2015. *Proceedings of the National Academy of Sciences of the United States of America*, *115*(49), 12401–12406. https://doi.org/10.1073/pnas.1812955115

Zhao, Y., Zhang, L., Pan, Y., Wang, Y., Paulot, F., & Henze, D. K. (2015). Atmospheric nitrogen deposition to the northwestern Pacific: Seasonal variation and source attribution. *Atmospheric Chemistry and Physics*, *15*(18), 10905–10924. https://doi.org/10.5194/acp-15-10905-2015

Zhao, Z.-Y., Cao, F., Fan, M.-Y., Zhang, W.-Q., Zhai, X.-Y., Wang, Q., & Zhang, Y.-L. (2020). Coal and biomass burning as major emissions of NO_x in Northeast China: Implication from dual isotopes analysis of fine nitrate aerosols. *Atmospheric Environment*, *242*, 117762. https://doi.org/10.1016/j.atmosenv.2020.117762

Zong, Z., Tan, Y., Wang, X., Tian, C., Li, J., Fang, Y., et al. (2020). Dual-modelling-based source apportionment of NO_x in five Chinese megacities: Providing the isotopic footprint from 2013 to 2014. *Environment International*, *137*, 105592. https://doi.org/10.1016/j.envint.2020.105592

Zong, Z., Tian, C., Li, J., Syed, J. H., Zhang, W., Fang, Y., et al. (2020). Isotopic Interpretation of Particulate Nitrate in the Metropolitan City of Karachi, Pakistan: Insight into the Oceanic Contribution to NO_x. *Environmental Science & Technology*, *54*(13), 7787–7797. https://doi.org/10.1021/acs.est.0c00490

Zong, Z., Tian, C., Sun, Z., Tan, Y., Shi, Y., Liu, X., et al. (2022). Dataset of nitrate in North China: Isotopic information from 10 offshore cruises in the Bohai Sea from 2014 to 2019 [Dataset]. Zenodo. https://doi.org/10.5281/zenodo.6420620

Zong, Z., Wang, X., Tian, C., Chen, Y., Fang, Y., Zhang, F., et al. (2017). First Assessment of NO_x Sources at a Regional Background Site in North China Using Isotopic Analysis Linked with Modeling. *Environmental Science & Technology*, *51*(11), 5923–5931. https://doi.org/10.1021/acs.est.6b06316

Zong, Z., Wang, X., Tian, C., Chen, Y., Fu, S., Qu, L., et al. (2018). PMF and PSCF based source apportionment of $PM_{2.5}$ at a regional background site in North China. *Atmospheric Research*, *203*, 207–215. https://doi.org/10.1016/j.atmosres.2017.12.013

Zong, Z., Wang, X., Tian, C., Chen, Y., Qu, L., Ji, L., et al. (2016). Source apportionment of $PM_{2.5}$ at a regional background site in North China using PMF linked with radiocarbon analysis: Insight into the contribution of biomass burning. *Atmospheric Chemistry and Physics*, *16*(17), 11249–11265. https://doi.org/10.5194/acp-16-11249-2016

References From the Supporting Information

Elliott, E. M., Yu, Z., Cole, A. S., & Coughlin, J. G. (2019). Isotopic advances in understanding reactive nitrogen deposition and atmospheric processing. *The Science of the Total Environment*, *662*, 393–403. https://doi.org/10.1016/j.scitotenv.2018.12.177

Fibiger, D. L., & Hastings, M. G. (2016). First Measurements of the Nitrogen Isotopic Composition of NO_x from Biomass Burning. *Environmental Science & Technology*, *50*(21), 11569–11574. https://doi.org/10.1021/acs.est.6b03510

Hastings, M. G., Jarvis, J. C., & Steig, E. J. (2009). Anthropogenic impacts on nitrogen isotopes of ice-core nitrate. *Science*, *324*(5932), 1288. https://doi.org/10.1126/science.1170510

Hastings, M. G., Steig, E. J., & Sigman, D. M. (2004). Seasonal variations in N and O isotopes of nitrate in snow at Summit, Greenland: Implications for the study of nitrate in snow and ice cores. *Journal of Geophysical Research*, *109*(D20), D20306. https://doi.org/10.1029/2004jd004991

Heaton, T. H. E. (2017). $^{15}N/^{14}N$ ratios of NO_x from vehicle engines and coal-fired power stations. *Tellus B: Chemical and Physical Meteorology*, *42*(3), 304–307. https://doi.org/10.3402/tellusb.v42i3.15223

Li, D., & Wang, X. (2008). Nitrogen isotopic signature of soil-released nitric oxide (NO) after fertilizer application. *Atmospheric Environment*, *42*(19), 4747–4754. https://doi.org/10.1016/j.atmosenv.2008.01.042

Miller, D. J., Chai, J., Guo, F., Dell, C. J., Karsten, H., & Hastings, M. G. (2018). Isotopic Composition of In Situ Soil NO_x Emissions in Manure-Fertilizes Cropland. *Geophysical Research Letters*, *45*(21), 12058–12066. https://doi.org/10.1029/2018gl079619

Shi, G., Chai, J., Zhu, Z., Hu, Z., Chen, Z., Yu, J., et al. (2019). Isotope fractionation of nitrate during volatilization in snow: A field investigation in Antarctica. *Geophysical Research Letters*, *46*(6), 3287–3297. https://doi.org/10.1029/2019gl081968

Shi, Y., Tian, P., Jin, Z., Hu, Y., Zhang, Y., & Li, F. (2022). Stable nitrogen isotope composition of NO_x of biomass burning in China. *The Science of the Total Environment*, *803*, 149857. https://doi.org/10.1016/j.scitotenv.2021.149857

Song, W., Liu, X.-Y., Hu, C.-C., Chen, G.-Y., Liu, X.-J., Walters, W. W., et al. (2021). Important contributions of non-fossil fuel nitrogen oxides emissions. *Nature Communications*, *12*(1), 243. https://doi.org/10.1038/s41467-020-20356-0

Walters, W. W., Tharp, B. D., Fang, H., Kozak, B. J., & Michalski, G. (2015). Nitrogen Isotope Composition of Thermally Produced NO_x from Various Fossil-Fuel Combustion Sources. *Environmental Science & Technology*, *49*(19), 11363–11371. https://doi.org/10.1021/acs.est.5b02769

Yu, Z., & Elliott, E. M. (2017). Novel method for nitrogen isotopic analysis of soil-emitted nitric oxide. *Environmental Science & Technology*, *51*(11), 6268–6278. https://doi.org/10.1021/acs.est.7b00592

Zhang, Z., Zheng, N., Liang, Y., Luo, L., Xiao, H., & Xiao, H. (2020). Dominance of Heterogeneous Chemistry in Summertime Nitrate Accumulation: Insights from Oxygen Isotope of Nitrate (delta O^{18}-NO_3^-). *ACS Earth and Space Chemistry*, *4*(6), 818–824. https://doi.org/10.1021/acsearthspacechem.0c00101

Zong, Z., Sun, Z., Xiao, L., Tian, C., Liu, J., Sha, Q., et al. (2020). Insight into the Variability of the Nitrogen Isotope Composition of Vehicular NO_x in China. *Environmental Science & Technology*, *54*(22), 14246–14253. https://doi.org/10.1021/acs.est.0c04749